ORIGINAL ARTICLE

Xenotransplantation **WILEY**

Large-gap peripheral nerve repair using xenogeneic transplants in rhesus macaques

Paul Holzer[1,2] | Elizabeth J. Chang[2] | Kaitlyn Rogers[2] | Jamie Tarlton[3] | Diana Lu[2] | Natasha Gillespie[3] | Jon Adkins[2] | Monica Metea[4] | Alan LaRochelle[5] | Joan Wicks[6] | Buket Onel[7] | Steve Gullans[2] | Joshua C. Doloff[1,8] | Linda Scobie[3] | Curtis L. Cetrulo Jr.[9,10] | Rod Monroy[2]

[1]Whiting School of Engineering, Johns Hopkins University, Baltimore, Maryland, USA

[2]XenoTherapeutics Inc., Boston, Massachusetts, USA

[3]Department of Biological and Biomedical Sciences, Glasgow Caledonian University, Glasgow, UK

[4]Preclinical Electrophysiology Consulting, LLC, Boston, Massachusetts, USA

[5]Biomedical Research Models, Inc. (Biomere), Worcester, Massachusetts, USA

[6]StageBio, Mt Jackson, Virginia, USA

[7]Xeno Diagnostics, LLC, Indianapolis, Indiana, USA

[8]Department of Biomedical Engineering, Translational Tissue Engineering Center, Johns Hopkins University School of Medicine, Baltimore, Maryland, USA

[9]Reconstructive Transplantation Laboratory, Massachusetts General Hospital, Boston, Massachusetts, USA

[10]Shriners Hospital for Children-Boston, Harvard Medical School, Boston, Massachusetts, USA

Correspondence
Paul Holzer, Whiting School of Engineering, Johns Hopkins University, Baltimore, MD 21218-2608, USA.
Email: pholzer1@jhu.edu

Curtis L. Cetrulo, Jr. and Rod Monroy are co-senior authors.

Abstract

Surgical intervention is required to successfully treat severe, large-gap (≥4 cm) peripheral nerve injuries. However, all existing treatments have shortcomings and an alternative to the use of autologous nerves is needed. Human and porcine nerves are physiologically similar, with comparable dimensions and architecture, presence and distribution of Schwann cells, and conserved features of the extracellular matrix (ECM). We report the repair of fully transected radial nerves in 10 Rhesus Macaques using viable, whole sciatic nerve from genetically engineered (GalT-KO), designated pathogen free (DPF) porcine donors. This resulted in the regeneration of the transected nerve, and importantly, recovery of wrist extension function, distal muscle reinnervation, and recovery of nerve conduction velocities and compound muscle action potentials similar to autologous controls. We also demonstrate the absence of immune rejection, systemic porcine cell migration, and detectable residual porcine material. Our preliminary findings support the safety and efficacy of viable porcine

nerve transplants, suggest the interchangeable therapeutic use of cross-species cells, and highlight the broader clinical potential of xenotransplantation.

1 | INTRODUCTION

Severe trauma to the extremities frequently results in neurotmesis, the complete transection of peripheral nerves, a devastating injury.[1,2] It is estimated that 20 million Americans suffer from peripheral nerve injury (PNI), resulting in nearly 50 000 surgeries annually.[1] Treatment of injuries ≥4 cm, termed large-gap PNIs, are especially challenging as direct co-aptation is only possible for smaller defects.[3,4] In such cases, a nerve conduit (NC) is needed. The use of autologous nerves, such as the sural, is considered the standard of care despite complications such as donor site morbidity, chronic pain, paresthesia, insufficient length, or improperly matched fascicular areas and patterns.[5,6] Alternatives such as allogeneic nerve transplants or synthetic, non-biological conduits exist,[7,8] but all current options have numerous shortcomings and outcomes are suboptimal.[2] Therefore, a reliable, high-quality, and widely available alternative is highly desirable in the repair of large-gap PNIs.[2]

The goal of surgical repair with NCs is to facilitate a complex, natural repair process, thereby maximizing the potential for the reinnervation of distal targets. Within 24 h of nerve trauma, an irreversible cascade of apoptosis known as Wallerian degeneration occurs, characterized by the dissolution of axonal cell membrane and cytoskeleton, release of axoplasm, retraction of the proximal and distal nerve stumps, and chromatolysis, the disruption of neurotransmitter production necessary for synaptic activity and axonal growth.[9] Schwann cells and macrophages phagocytose myelin and axon debris and release neurotrophic growth factors, such as GDNF, NT-3, and NGF, creating a microenvironment favorable for axonal repair.[10] Despite degradative protease activity, basal laminae are spared, leaving channels formed from residual endoneurial structures to direct an axonal growth cone emerging from Nodes of Ranvier at the proximal site towards a downstream synaptic target. Components of the conserved extracellular matrix (ECM), such as transmembrane cell adhesion molecules, laminin, fibronectin, and glycosaminoglycans (GAGs), provide stimulation of neuronal activity, Schwann cell migration,[11] and modulation of neurite extensions resulting in regeneration at a rate of 1–2 mm/day.[2,12]

In the repair of large-gap PNIs, many conduits are unsuitable[2,13,14] due to mechanistic limitations. An unguided growth cone will result in a disorderly axonal mass forming a neuroma, a clinically painful outcome.[15] Optimal nerve conduits should contain a matrix-rich ECM scaffold, Schwann cells, neurotrophic growth factors, and a fascicular area comparable to or greater than that of the injured native nerve. Material properties such as plasticity, durability, and tensile strength should be sufficient to resist mechanical injury.[5,10,16] In addi-

tion, research indicates that return of perfusion is critical, as diffusion of oxygen, nutrients, and cytokines relies on a network of longitudinally arranged blood vessels that courses throughout the nerve.[17] Therefore, vasculature that can be co-opted to restore perfusion would be advantageous.[18] Lastly, manufacturing ability, storage, and clinical acceptability are other critical considerations.

Viable xenogeneic nerve transplants offer the potential for a biological nerve conduit comprised of mixed-modal nerves, which can facilitate nerve recovery in large-gap PNIs and also support efferent and afferent conduction through the conduit without the additional morbidity and paresthesia from self-harvest and limitations of clinical availability.

Previously, the use of wild-type xenografts was explored, yielding mixed results. Evans et al.[19] reviewed all published research on xenograft nerve repair from 1880 to 1991, spanning more than 40 studies and hundreds of human and non-human subjects in which nerve sources were predominantly dogs, rabbits, and rodents. However, general optimism for xenografts diminished after research and experience demonstrated inferior outcomes when compared to autografts,[14,20] as well as undesirable immunological responses.[19,21–23] The adverse immunological responses are better understood in the case of human recipients, primarily mediated by preformed antibodies against Galactose-α-1,3-galactose (α-Gal), an oligosaccharide expressed on all non-primate mammalian cells.[24] In some instances, xenografts were decellularized to diminish the rejection phenomenon as well as the possibility of zoonosis, but this resulted in the loss of essential cell populations in the process.[2]

Surprisingly, few of these studies investigated the potential of porcine nerves, given the greater physical and genetic similarities between *Sus Scrofa* and *Homo Sapiens*. Recently interest in the use of porcine donors has gained momentum, but limited research exists in this area. The similarity of critical physiological characteristics between pig and human nerves, including size, length, architecture, and extracellular matrix composition,[1,25–28] would suggest the potential for regenerative capacity.

Genetic engineering of porcine donors as well as mitigation strategies and possible treatments for zoonosis, have made clinical xenotransplantation a more achievable goal.[21,24,29–33] Thus, we hypothesized that instead of traditional xenografts, viable xenogeneic nerve transplants derived from specialized, Designated Pathogen Free (DPF), GalT-KO porcine donors could offer an alternative solution for repair of large-gap (≥4 cm) PNIs.

Here, in a two-phase, 12-month pilot study, we report successful axonal regeneration, distal muscle reinnervation, and recovery of

conduction velocity following surgical repair of fully transected radial nerves in 10 Rhesus Macaque recipients via the use of xenogeneic nerve transplants.

2 | METHODS

2.1 | Animals

This study's surgical procedures, protocols, and guidelines for animal care were independently IACUC reviewed and monitored to ensure the ethical treatment of animals. The Test Facility is accredited by the Association for the Assessment and Accreditation of Laboratory Animal Care, International (AAALAC) and registered with the United States Department of Agriculture (USDA) to conduct research on laboratory animals. The veterinary care of the animals were in accordance with the protocol, Test Facility's SOPs, and regulations outlined in the applicable sections of the Final Rules of the Animal Welfare Act regulations (9 Code of Federal Regulations [CFR] Parts 1, 2, and 3), the Public Health Service Policy on Humane Care and Use of Laboratory Animals, the Guide for the Care and Use of Laboratory Animals, the U.S. Food and Drug Administration (FDA) Good Laboratory Practice (GLP) regulations, standards, and guidelines (US-FDA 21 CFR Part 58.351 and Guidance for Industry [GFI] 197), in accordance with ARRIVE guidelines, and the Biomere, Policy on Humane Care. The protocol and any amendments or procedures which involved the care or use of animals in this study were reviewed and approved by the Test Facility's Institutional Animal Care and Use Committee (IACUC) before the initiation of such procedures.

All xenogeneic nerve transplants used in this study were sourced from a single genetically engineered α-1,3-galactosyltransferase knockout (GalT-KO), PCMV negative, designated pathogen free (DPF) porcine donor.[34] Five male and five female naïve Rhesus Macaques (Macaca mulatta) served as xenogeneic nerve transplant recipients.

2.2 | Cryopreservation

Following procurement, nerve xenotransplants were prepared via standardized institutional protocol where the nerve was packaged in cryovials (Simport, T310-1A, Beloeil, QC) and cryoprotective media (5 ml, CryoStor CS5 media, BioLife Solutions, Bothwell, WA) was added to each vial before it was sealed. Cryopreservation was achieved via a controlled rate, phase freezer at a rate of 1°C per minute to −40°C, and then rapidly cooled to a temperature of −80°C. Fresh nerve xenotransplants were stored in RPMI 1640 media and maintained at 4°C until use (24–48 h).

2.3 | Surgical procedures

The porcine sciatic nerve was selected as the source of the xenogeneic transplant due to its superstructural similarity to human and primate

nerves.[1] The radial nerve was selected as the transplantation recipient site because there are minimal neighboring nerves. Those in close proximity may reinnervate downstream muscle fibers and complicate electrophysiology and functional analysis of the extensor digitalis muscles. Transplantation at the radial nerve also allowed for ethical loss of function and clearly articulated return of function in an observable and isolated movement. The maximum practical gap size possible was 4 cm based on the measured lengths of the recipients' limbs. The mean distance from the recipients' proximal neurorrhaphy site to the site of innervation of the extensor carpi radialis longus and extensor carpi radialis brevis muscles measured 15.7 ± 0.17 cm.[35]

The porcine donor was euthanized and prepared for surgery as previously described.[34] To isolate the sciatic nerve prior to harvesting, a linear incision was made midway between the sacrum and the ischium and extended ventrally along the posterior aspect of the femur, longitudinally dissecting the gluteus medius, gluteus maximus, piriformis, and biceps femoris muscles, to the proximal tibiofibular joint. The sciatic nerve was visualized and harvested by radial transections distal to the nerve origin and proximal to the bifurcation into the tibial and common peroneal nerves. This process was repeated on the bilateral side.

Two porcine sciatic nerves were harvested from one donor (Figure 1a), trimmed into ten x 4 cm segments (Figure 1b). Five sciatic nerve segments were stored in RPMI 1640 media (ThermoFisher Scientific, Waltham, MA) and maintained at 4°C until surgical use 24–48 h later. The second set of five porcine sciatic nerves were cryopreserved per protocol, and stored at −80°C for a period of 7–8 days, after which they were thawed as previously described.[36] This cryopreserved nerve was used as the source of the donor nerve to repair the radial nerve defects in the remaining five Rhesus Macaque recipients 7–8 days later. Cryopreservation of the sciatic nerve was necessary to limit variability of surgical personnel, techniques, and conditions, as the number of surgeries and availability of surgical team required more than one series of surgical operations.

To avoid potential necrosis in the central portion of a nonvascularized, large-caliber nerve transplant, the porcine nerve transplants were selected during surgery from regions of the naturally tapered sciatic nerve, which closely matched the caliber and diameter of the proximal and distal radial nerve end in the nonhuman primate. Prior to transplantation, xenogeneic nerves were trimmed to 4 cm to fit the defect size.

Bilateral, 4 cm complete transections of radial nerves were surgically introduced in a total of ten Rhesus Macaque recipients. Recipients, under anesthesia,[37] were positioned in lateral recumbency with the shoulder at 90° flexion, full internal rotation, and neutral abduction. The subcutaneous tissue and deep fascia were dissected for anatomical orientation. A 6–8 cm skin incision was made along the posterolateral margin of the proximal arm towards the antecubital fossa. This procedure exposed the long and lateral heads of the triceps, which converged to form the triceps aponeurosis.[38] The intramuscular plane between the long and lateral head of the triceps was developed approximately 2.5 cm proximal to the apex of the aponeurosis, where the radial nerve and accompanying vessels were observed against the humerus in the radial groove. The surgical plane was extended proximally and distally
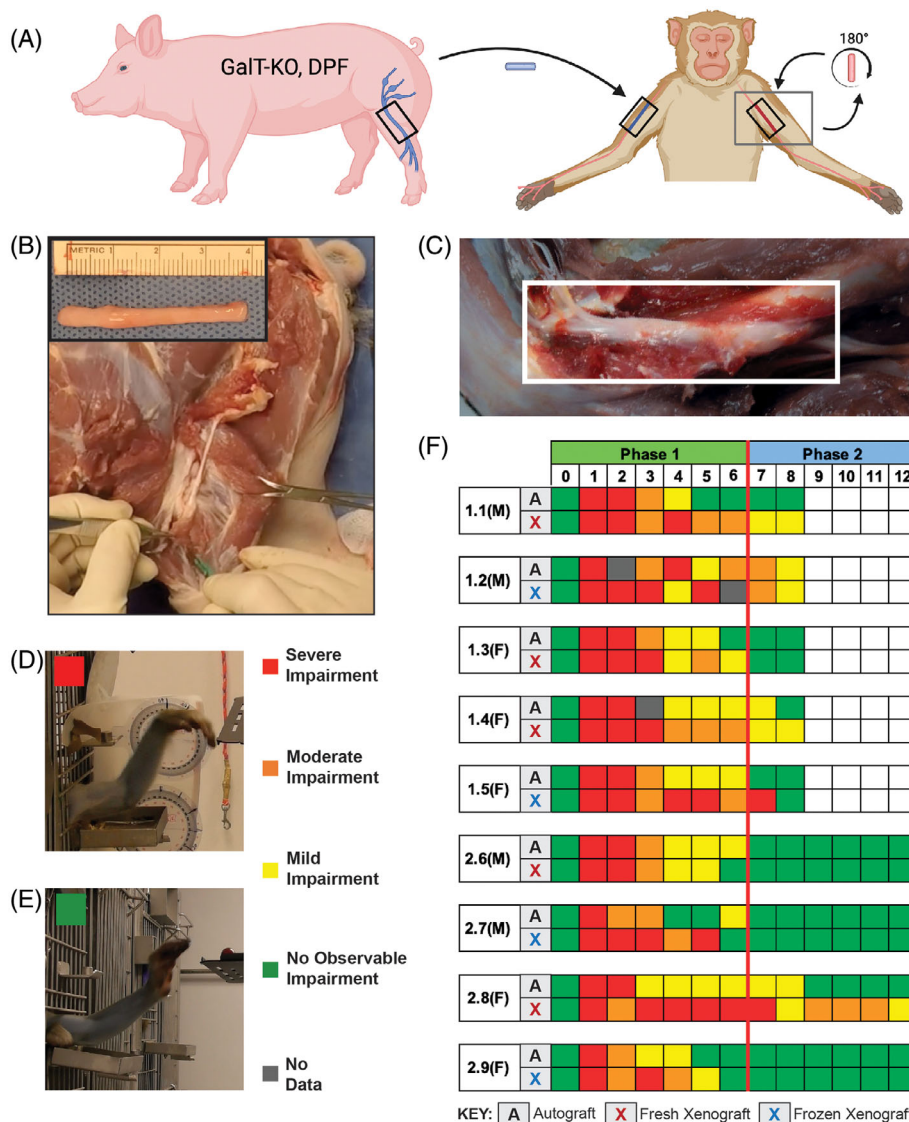
FIGURE 1 Experimental study design. (A) Schematic of experimental study design. Porcine sciatic nerve was trimmed to 4 cm and used to repair the complete transection of the radial nerve in 10 Rhesus Macaque recipients. In the contralateral arm, the transected, autologous radial nerve is rotated 180° and reimplanted as a control. (B) Visualization of porcine sciatic nerve in situ during procurement surgery. Inset shows trimmed nerve (4 cm). (C) Representative image of the reconstructed radial nerve from a limb treated with the xenogeneic transplant, photographed at necropsy (12- months postoperative). (D and E) Recovery of wrist extension function was qualitatively assessed from monthly video recordings by an analyst blinded to the transplant type. Top image (D) depicts severe impairment, lower image (E) depicts no observable impairment. (F) Magnitude of recovery of wrist extension function is illustrated via a heat map. Month 0 indicates baseline values for all graphs and heat maps. Phase 1 and 2 are separated by a line indicating variation in tacrolimus treatment. Numbers in the boxes to the left indicate specific subjects and their respective genders. The letter 'A' represents autologous treated limbs, while the letter 'X' in red represents fresh xenogeneic treated limbs and the letter 'X' in blue represents frozen xenogeneic treated limbs.

to minimize unintended injury. The radial nerve was distally transected approximately 1 cm proximal to the origin of the deep branch. A 4 cm segment was removed to create the defect and saved for reattachment or subsequent analysis. Nerve transplants were attached proximally and distally with four to eight equidistant 8-0 nylon monofilament sutures at each neurorrhaphy site. The incision was then closed in layers using subcuticular, absorbable sutures.

This process was performed bilaterally per each of the ten recipients; both xenogeneic and autologous nerves were transplanted in the same surgical procedure. Limb designation (right/left) for xenogeneic or autologous transplants was randomly assigned and blinded from observers for analysis. In the contralateral arm, excised Rhesus Macaque radial nerve segments were rotated 180° and reimplanted as a surgical control (Figure 1a).[2] The 10 recipients were randomly, evenly divided between two surgical series, one week apart (Table S1). Surgeries were performed synchronously, and the surgical personnel, sterile field, surgical technique, and uniformity of the transplant procedure were independently assessed for quality control at each step.

2.4 | Immunosuppression

Intramuscular injection of tacrolimus, at a dosage of 0.15 mg/kg/day, began 10 days before surgery and was continued until 8-months for Group 1 (N = 5) and 6-months for subjects in Group 2 (N = 5) as previously described.[39] Trough levels were maintained between 20 and 30 ng/ml. Dosing for subjects experiencing levels above or below the range was adjusted to bring the trough level within the target range.

2.5 | Pathology

At the designated necropsy time point, the animals were sedated with Ketamine (10–15 mg/kg, Intramuscular [IM]). An IV catheter was placed, and euthanasia was performed by administration of Eutha-sol (≥50 mg/kg or to effect, IV). Explants of the entire autologous or xenogeneic transplant, including proximal and distal nerve, as well as samples of spleen, liver, kidney, lung, and heart were collected, fixed in 10% neutral buffered formalin, and transferred to 70% ethanol after approximately 72 h. Nerve explants were trimmed longitudinally, routinely processed, and embedded in paraffin blocks. A cross section across the graft was not taken and processed. Resulting blocks were sectioned, and stained with either hematoxylin and eosin (H&E), Luxol Fast Blue (LFB), or immunohistochemically stained for neuro-filament H (NF-H). Spleen, liver, kidney, and heart were trimmed, processed, embedded in paraffin, sectioned and stained with H&E. All tissues were evaluated in a manner blinded to treatment and scored by a pathologist. Nerve explants were evaluated for morphologic changes and underwent semi-quantitative scoring (Table 1). All measurements of axon diameter were made by the pathologist using an ocular micrometer. For histopathology, explanted tissues were stained by immunohistochemistry for expression of Neurofilament H to identify axons. Luxol Fast Blue staining was used to demonstrate myelination levels of the various regions of the explant. Inflammation was scored by the pathologist based upon the presence of infiltrating lymphocytes, macrophages and histiocytes on H&E stained slides.

At necropsy, samples of the spleen, liver, kidney, and other organs were also collected and stored at −80°C.

TABLE 1 Histopathology evaluations scoring parameters

Score	Nerve bundle diameter (μm)	Myelination
0	No nerve	No detectable myelin
1	<100	Minimal myelin
2	101–200	Moderate myelin
3	201–300	Significant myelin
4	>300	Fully myelinated

Qualitative histological scoring of nerve bundle diameter, and myelination.

2.6 | DNA and RNA extraction and PCR detection of porcine and primate cells

PERV copy number and expression were analyzed by Q-PCR to assess the presence of PERV DNA and mixed chimerism. Samples analyzed included xenogeneic and autologous nerve tissues harvested at 8- and 12-months postoperative, sera and PBMCs from the nine subjects obtained at various time points over the 12-month study, and spleen, kidney, liver, heart, and lung samples obtained at necropsy.

Twenty milligrams of the xenogeneic porcine tissue samples and 7 mg of autologous primate tissue samples were treated with the DNeasy Blood and Tissue Kit (Qiagen, Crawley, UK) as described by the manufacturer that included the RNase A-treatment step. The isolated DNA was quantified by UV spectrophotometry. Quantitative PCR amplification of 18S (Eurogentec, Seraing, Belgium) was carried out to assess the DNA homogeneity across samples. Serum samples were processed using the Viral RNA mini kit (Qiagen, Crawley, UK) as described by the manufacturer incorporating the DNA digestion step using DNase I to isolate viral RNA. Samples were then processed using the RNeasy MinElute Cleanup kit (Qiagen, Crawley, UK). All Serum samples were shown to have an Internal Positive Control (IPC) CT <32 progressed to PERV transcription analysis. PMBC samples were processed for DNA isolation using a modified version of the manufacturers "Whole Blood" protocol for the Gentra Puregene Blood kit (Qiagen, Crawley, UK). The modified protocol involved homogenizing the PBMC samples prior to RNase A treatment, protein precipitation and, finally, isopropanol and 70% ethanol washes were added before DNA hydration. The DNA product was quantified using UV spectrophotometry and 18S amplification carried out to assess DNA homogeneity between samples while using 200 ng/reaction. PBMC samples shown to have an 18s CT <27 progressed to PERV copy number and mixed chimerism analysis. At necropsy, tissue samples of the kidney, liver, lung, and spleen were harvested. RNA isolation was conducted on 35 mg of the tissue samples using the RNeasy mini kit (Qiagen, Crawley, UK) with homogenization using a Fast-Prep 24 (MP Biomedicals, Eschwege, Germany). The RNA product was quantified using UV spectrophotometry and 18S amplification was carried out to assess DNA homogeneity between samples while using 200 ng/reaction. Tissue samples were shown to have an 18S CT <13 progressed to amplification, reverse transcription, and PERV copy number and mixed chimerism analysis.

Amplification was carried out using an Applied Biosystems ViiA 7 Real-Time PCR System with a polymerase activation step (10 min at 95°C) and 40 amplification cycles of 15 s at 95°C, 30 s at 53°C, and 30 s at 60°C. All primate and porcine transplantation site samples shown to have an 18s CT <29 progressed to PERV copy number and mixed chimerism analysis. PERV genome copy number quantification and mixed chimerism was assessed by quantitative PCR (Q-PCR) using the QuantiTect virus kit (Qiagen, Crawley, UK), with identical cycling conditions described above. PERV was assessed using TaqMan primers specific to the PERV-pol gene as previously described.[40] PERV quantification was carried out by comparison to standards of known PERV copy numbers. The limit of quantification (LOQ) for PERV using this

assay is ten copies per reaction. Mixed chimerism was assessed using TaqMan primers for porcine centromeric DNA that were also used in the study described.[40] Detection of porcine cells was quantified by comparison to standards of known porcine cell content. The LOQ for porcine cells using this assay is 0.026 cells per reaction.

Qualitative PCR for the reference gene RPL13A (ribosomal protein gene) was carried out to confirm that DNA was suitable for amplification. Primers used were 5′-CCT GGA GAA GAG GAA AGA GA-3′ and 5′-TTG AGG ACC TCT GTG TAT TTG TCA AG-3′ giving an amplicon of 126 bp. Fifty nanograms of DNA and 0.5 μM primers in a total volume of 25 μl were cycled under the following conditions: 5 min at 94°C, 50x (10 s at 94°C; 15 s at 58°C; 15 s at 72°C) 10 min at 72°C. This PCR will detect both primate and porcine material.

Detection of primate-specific DNA was carried out using qualitative PCR as described previously with modifications.[41] In brief, the primers used were P5 5′-ATC TGG ACC AGA AAT CCC GAC GAT ATT ACT AAT GAG GAG-3′ and P6 5′-CTT GTA GTT CTC

TTT ATC TTC CGC CAG TTC AGT AAA GAG-3′, giving an amplicon of 450 bp. Using the Taq PCR core kit (Qiagen, Surrey, UK) 75 ng of DNA and 0.2 μM primers in a total volume of 50 μl was cycled under the following conditions; 94°C for 5 min, 40x (30 s at 94°C, 30 s at 5°C, and 60 s at 72°C), 10 min at 72°C. PCR analysis was preferred for specificity which is not seen by the use of antibodies to nerve components.

All samples were confirmed positive for either the internal positive control (sera) or the control reference genes indicating the validity of the analysis.

2.7 | Electrophysiology

Nerve conduction studies (NCS) are non-invasive electrodiagnostic techniques used commonly for functional tests of the peripheral nervous system. Nerve injury or regeneration is evaluated by testing the ability of the nerve to conduct an electrical impulse. The technique involves recording electrical activity at a distance from the site where a propagating action potential is induced in a peripheral nerve. The nerve is stimulated at one or more sites along its course, and the electrical response of the nerve is recorded using the same instrument.

All recordings were performed at Biomere (Worcester, MA). All signal collections and post-collection data analyses were performed with a vendor-calibrated and certified clinical electromyography (EMG) machine (Natus Neurology System with Synergy software), per Preclinical Electrophysiology Consulting SOPs. Subdermal platinum needle recording electrodes were used for recording (e.g., 0.703, 30-mm, 22G3, 1.25 in). A Natus pediatric stimulator was used for stimulation in order to maintain consistent distance between the cathode and the anode. During all recording sessions animals were lightly anesthetized by facility staff, following Biomere SOPs, and placed on a temperature-controlled warm pad. Animals were sedated with Ketamine (10–15 mg/kg) or Telazol (5–10 mg/kg, IM) or Ketamine and Dexdomitor (~7.5 and 0.02 mg/kg mixture, IM. The anesthesia provided adequate sedation for handling while preserving peripheral evoked responses. Body temperature was recorded.

Signal measurement marks placed automatically by the software were manually verified post-collection. Onset latency was measured from the stimulus artifact to the initiation of the depolarization to the nearest 0.01 ms; amplitude was measured from baseline to the peak of the depolarization to the nearest 0.01 μV for sensory responses, and to the nearest 0.01 mV for motor responses. Group summaries were calculated with MS Excel. Differences in measures across groups were compared using Student's t-Test.

Nerve conduction was assessed for the radial motor and radial sensory branches. These measurements detected recovery of function at locations along the nerve. F-wave responses were tested at the last timepoint. All recording procedures were adapted from routinely used neurological clinical protocols. Locations for stimulation and recording were located relative to anatomical landmarks (e.g., elbow, spiral groove, axilla). An additional stimulation was elicited directly over the graft. Orthodromic compound muscle action potentials were elicited in the radial motor nerve and antidromic sensory nerve action potentials were elicited in the radial sensory nerve. Orthodromic and antidromic stimulations were relative to the physiological conduction in the respective nerves, per clinical conventions.

For sensory branches, the recording electrode was positioned directly over the distal branches of the nerve and sensory nerve action potentials (SNAPs) were elicited. For radial motor branches the recording electrode was positioned over the belly of the extensor digitorum communis muscle (EDC; innervated by the radial nerve) in a belly-tendon montage, and compound muscle action potentials (CMAPs) were elicited. The recording location was at the junction of the upper third and middle third of the forearm.

2.8 | Nerve conduction velocity and functional evaluation

The Nerve Conduction Velocity (NCV) measurement is the velocity of the fastest fibers present in the nerve bundle tested. Decreased conduction velocity is assumed due to both axonotmesis (axonal loss) and neurapraxia (conduction block). Conduction velocity slowing alone, without conduction block, does not necessarily produce clinical weakness if sufficient motor units remain innervated. The presence of nerve conduction does not necessarily indicate fully functional muscle innervation. Uneven conduction within the nerve may indicate localized areas of demyelination, remyelination with immature myelin, loss of fibers, or connective tissue blockages. Qualitative regain of radial nerve functionality was monitored according to the following categorical scale: no observable impairment, mild impairment, moderate impairment, and severe impairment.

2.9 | Functional assessment

A previously reported radial nerve injury model was adapted to assess the functional recovery of xenogeneic and autologous nerve transplant recipients.[42] Radial nerve injury proximal to the elbow results in a loss of wrist extension function, or "wrist drop," loss of forearm muscle

tonality, and digital extension due to motor denervation of the extensor carpi radialis longus and extensor carpi radialis brevis muscles.[43,44] Wrist extension testing and evaluation were performed monthly. Subjects were offered a food treat outside of the of the cage in a manner to encourage them to reach out to grab it with a wrist angle extension required. This is done with one hand then the other. The test was videotaped for subsequent analysis. Analysis was performed by a scientist blinded to the type of nerve used. The neutral position was in line with the forearm, 0º. Angle data were recorded then converted to a range of motion descriptive classification for every 30º of wrist flexion. The ROM score was defined as: angles less than 31º (No observable impairment), 31º–60º (Mild Impairment), 61º–90º (Moderate Impairment), and >91º (Severe Impairment).

2.10 | Measurement of immunoglobulins

Total serum IgM and IgG were measured using a commercial ELISA, IgG, and IgM ELISA kits from Life Diagnostics following manufacturer's instructions. Overall median and IQR values were determined in all nine animals included in the study.

Binding of the xenoreactive antibody to pig cells was measured as previously described.[45] Cryopreserved genetically modified α-1,3-galactosyltransferase knockout (GalT-KO) porcine PBMCs were thawed, and cell concentration was determined using Coulter MD II (Coulter Corporation, Miami, FL). Cells were diluted to a concentration of 1.5×10^6 cells/ml in FACS buffer (1X Hanks' Balanced Salt Solution (HBSS) with calcium and magnesium, 0.1% Body Surface Area (BSA), and 0.1% sodium azide). Decomplementation of the serum samples was carried out by heat inactivation for 30 min at 56°C and diluted at 1:2, 10, 100, 1000, and 10 000 ratios using FACS buffer. A total of 100 μl of the cells were added into each well in 96-well u-bottom plate with 10 μl of the diluted serum samples and incubated for 30 min at 4°C. Cells were washed one time using 200 μl FACS buffer. To prevent nonspecific binding, cells were incubated in 100 μl 10% goat serum for 10 min at room temperature, followed by one more additional washing. Cells were stained with goat anti-human IgG PE and goat anti-human IgM FITC (Jackson ImmunoResearch Laboratories Inc., West Grove, PA) for 30 min at 4°C. Cells were washed two times using FACS buffer and resuspended in 200 μl 0.5% PFA in MACS/1X PBS buffer. Flow cytometric analysis completed on Novocyte flow cytometer (ACEA Biosciences, Inc. San Diego, CA). Flow cytometry data was analyzed using NovoExpress 1.3.0 (ACEA Biosciences, Inc.). Binding of anti-porcine IgM and IgG was assessed using Median Fluorescence Intensity (MFI) and relative MFI was obtained as follows: Relative MFI = Actual MFI value/Limit of Blank (MFI obtained using secondary antibody only in the absence of serum).

2.11 | Statistical analysis

The study design includes several acknowledged limitations that introduced variability between subjects and the non-normality of these data. As a result, a detailed statistical analysis is not appropriate for these findings.

2.12 | Hematology and clinical chemistry

Blood samples were obtained monthly and processed for serum or transferred to the Biomere Testing Facility laboratory and processed. Whole blood hematology samples were transferred to the Testing Facility laboratory. Whole blood was analyzed on an IDEXX Procyte analyzer for erythrocyte count, hemoglobin, hematocrit, platelet count, leukocyte count, reticulocyte count, and mean corpuscular volume, hemoglobin and hemoglobin concentration. Serum samples were analyzed using an IDEXX Catalyst analyzer (Chem15, Lyte4, Trig, and AST slides for A/G ratio, alanine aminotransferase, albumin, alkaline phosphatase, aspartate aminotransferase, calcium, chloride, cholesterol, creatinine, gamma-glutamyl transferase, globulin (by calculation), glucose, inorganic phosphate, potassium, sodium, total bilirubin, total protein, triglycerides, and urea nitrogen.

3 | RESULTS

3.1 | Clinical outcome

All 10 subjects tolerated the surgical procedure resulting in the complete loss of radial nerve function bilaterally (Figures 1a–c). Nineteen of the 20 surgical transplant procedures were successful. In one subject, histomorphological analysis at necropsy revealed a large neuroma proximal to the transplantation site as well as the lack of axonal continuity through and distal to the transplant indicating failure to maintain coaptation at the proximal anastomotic site. Thus, all functional, electrophysiological, and morphological data for both of the transplant types from this subject were removed from nerve analyses, but clinical data were retained to assess immunological and toxicological outcomes.

Over the entire course of the study, no adverse events, negative veterinary observations, or other deleterious systemic effects attributable to the xenotransplant were observed in any subject. At necropsy, there were no abnormal findings during inspection of internal organs and other tissues in any recipient, regardless of treatment and tacrolimus regimen. Hematology and chemistry analysis were monitored on a monthly basis and were within normal ranges.[35,46] Red blood cell (RBC), platelet (PLT) counts, hemoglobin (HGB), mean corpuscular volume (MCV), hematocrit (HCT), urea nitrogen (BUN), creatinine (CREA), and electrolyte levels were unremarkable for all subjects.[47,48]

In Phase 1, during which all 10 subjects received 0.15 mg/kg/day of intra-muscular tacrolimus for the first 6 months of the study, no serious adverse side effects, such as diarrhea, cachexia, or other effects were observed in any of the 10 subjects. Postoperative trough levels for the first 6 months were maintained in the range of 20–30 ng/ml, at times trough levels of individual recipients varied (4.9–32.2 ng/ml) and the

levels were adjusted to within target range with subsequent change in dosing.

In Phase 2 (post 6 months), during which five subjects continued the regimen (Group 1), and five subjects ceased tacrolimus treatment (Group 2), gradual weight increase was observed in Group 2 recipients, and all survived without incident to the 12-month end of study.

However, subjects in Group 1 presented with progressing symptoms associated with tacrolimus toxicity,[49] such as limited mobility in knee joints, muscle rigidity, stiffness, and atrophy, as well as significant weight loss. As a result of the tacrolimus-associated toxicity, at 8-months, the five subjects in Group 1 were euthanized.

3.2 | Functional evaluation

Radial nerve functional assessments were performed monthly for each recipient and included chair and cage-side observations of active and passive wrist angle flexion during the recipient's retrieval of objects requiring wrist angle extension to obtain them. A series of wrist extension and gripping attempts by each recipient were video recorded, for each isolated arm, for each month. Observations were performed using food treats or mechanical stimulation to encourage wrist extension and gripping. This resulted in 16:13:33 h of data, for 18 limbs of nine Rhesus Macaque transplant recipients. Over the entire study period, a combined 2057 total events were recorded. Results were analyzed by two independent investigators in a blinded manner with respect to the transplant type and location.

At least two stimulation locations are necessary for accurate assessment of motor nerve conduction, in order to account for delays introduced by the neuromuscular junction. In this study the NCV was expected to vary across the length of the nerve with progressive recovery and therefore stimulation was performed with a pediatric stimulator at four locations proximal and distal from the graft (e.g., lateral from the ulna or biceps tendon in the antecubital fossa; at the spiral groove; across the graft; and at the axilla between the coracobrachialis and the long head of the biceps). The nerve conduction velocities were averaged across the entire length of the nerve. Slightly different Left vs Right measurements are common.

The motor conduction velocity for each segment was calculated using the differences in onset latency and distance between each two points of stimulation along the radial nerve following supramaximal stimulation. The amplitude of the CMAP was determined at the peak of the response following supramaximal stimulation of the associated nerve. Segmental conduction velocities across the radial nerve were averaged.

For sensory stimulation, the stimulus strength was progressively increased until a response was evoked, and then increased further until a supramaximal response was elicited. Approximately 10 supramaximal stimuli were averaged for each sensory nerve. Sensory recordings were performed directly over the radial sensory nerve as it passes over the extensor pollicis longus tendon. Stimulation was performed over the radial side of the forearm, approximately 5 cm proximal to the recording site.

The distance from the recording site to the stimulation cathode was entered in the instrument during collections, for each site, and the conduction velocity was calculated by preset software protocols using the onset latency of the response and the distance (for sensory NCV) or the distance difference (for motor NCV calculations).

F-waves were elicited at the elbow, distal from the graft. F-waves are late responses attributed to the antidromic activation of anterior horn motor neurons following peripheral nerve stimulation, which then results in orthodromic impulses returning along the involved motor axons (also known as "backfiring of axons"). F-waves test motor conduction over long neuronal pathways including the proximal spinal segments and the nerve roots. The latency and amplitude of F-waves are known to vary, and multiple stimulations (8–10) were performed to ensure a response. F-wave responses under 20 ms indicated the presence of motor conduction over long neuronal pathways.

Qualitative regain of radial nerve functionality was monitored according to the following categorical scale: no observable impairment, mild impairment, moderate impairment, and severe impairment. Following surgery, complete loss of radial nerve function was observed bilaterally in all recipients regardless of nerve transplant type used. During Phase 1, the rate of recovery averaged across the recipients appeared to be slower in the xenogeneic transplanted limbs for both study groups (Figures 1d–f), while the overall magnitude of functional recovery was near equivalent between the limbs treated with xenogeneic nerve transplant and the autologous surgical control. Mild impairment was noticed in one autologous and three xenogeneic transplant arms at observational endpoints.

However, at the respective endpoints in Phase 2, there was no qualitative difference in the overall magnitude of functional recovery between limbs treated with a xenogeneic nerve transplant and the autologous control (Figure 1f). Subjects in group 2 showed a functional recovery after 6 months and 2 of the 4 received frozen nerves. Therefore, this recovery in phase 2 was regardless of whether the porcine nerve had been grafted fresh or frozen nerves.

3.3 | Electrophysiology

For all 18 limbs, preoperative median motor nerve conduction velocity was 64.26 m/s with an interquartile range (IQR) of 0.66 (Figure 2a), and median sensory nerve conduction velocity was 53.72 m/s (IQR = 0.11) (Figure 2b).

In Phase 1, at the first postoperative assessment (5-months), there was an overall reduction in median nerve conduction velocities to 36.50 m/s (IQR = 12.17) for autologous treated limbs, and 50.33 m/s (IQR = 21.16) for xenogeneic treated limbs. In sensory nerve, conduction velocity dropped to 25.00 m/s (IQR = 13.50) in limbs with the autologous control, and 22.00 m/s (IQR = 4.50) with the xenogeneic transplant.

In Phase 2, at 8-months postoperative, median motor nerve conduction velocity increased to 56.33 m/s (IQR = 13.01) autologous, and 57.00 m/s (IQR = 11.83) xenogeneic, indicating partial remyelination of
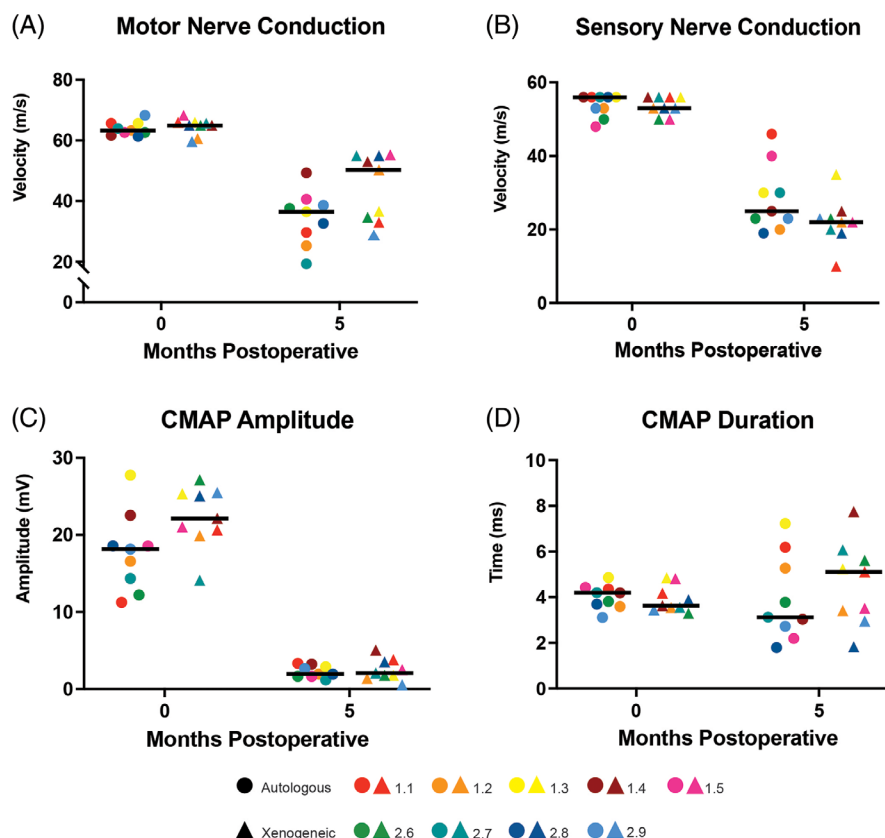
FIGURE 2 Phase 1 electrophysiological data. (A) Motor nerve conduction velocity showed partial recovery in all subjects, with the limbs treated with the xenogenic transplant exhibiting greater recovery. Circles represent autologous treated limbs, while triangles represent xenogeneic treated limbs. Each color represents an individual subject's data. (B) Sensory nerve conduction velocity values were similar between limbs treated with xeno-or-auto nerve transplants and demonstrated only partial recovery compared to preoperative levels. (C) At 5-months, compound muscle action potential (CMAP) amplitudes remained below the critical firing threshold in all limbs. (D) CMAP duration values were widely varied between subjects; however, mean CMAP durations for each transplant type returned to baseline by month 5.

fast-conducting fibers had occurred (Figure 3a). However, median sensory nerve conduction velocity did not return to preoperative baseline levels, only reaching 27.00 m/s (IQR = 12.5) autologous, and 27.00 m/s (IQR = 7.5) xenogeneic (Figure 3b).

At 12-months postoperative, the remaining four recipients in Group 2 demonstrated an increase in median motor nerve velocity to 62.17 m/s (IQR = 8.76) and 63.34 m/s (IQR = 4.33) autologous and xenogeneic treated limbs, respectively (Figure 3a). Sensory nerve conduction velocity remained stable at 25.50 m/s (IQR = 4.00) for the autologous treatment group and 27.5 m/s (IQR = 3.00) in the xenogeneic experimental group (Figure 3b).

Median preoperative CMAP amplitudes for all 18 limbs was 20.03 mV (IQR = 4.54). At 5-months, a nearly complete loss of action potential was observed in all limbs: 1.93 mV (IQR = 1.41) autologous, and 2.05 mV (IQR = 2.08) xenogeneic, levels at which nerves would be unable to reach threshold firing levels (Figure 2c). At 8-months, CMAP amplitudes for the autologous nerve transplants had recovered to 9.20 mV (IQR = 4.27), compared to a CMAP of 7.30 mV (IQR of 6.13) xenogeneic (Figure 3c). However, at 12-months, median CMAP amplitude magnitudes increased for both types of transplants, 15.44 mV (IQR = 4.64) for autologous, and 14.15 (IQR = 4.83) for xenogeneic.

Median preoperative CMAP duration values for all 18 limbs were 3.98 mV (IQR = 0.12) (Figure 2d). At 5-months, median durations were measured at 3.14 mV (IQR = 3.27) for autologous treated limbs, and 5.12 mV (IQR = 2.66) for limbs treated with the xenogeneic nerve transplant. Over the course of the study, however, maximum recovery was observed at 8-months postoperative, 4.81 mV (IQR = 1.71) autologous; 4.62 mV (IQR = 1.99), xenogeneic (Figure 3d). No major qualitative differences were observed in xenogeneic transplant vs autograft electrophysiology (Table S2).

3.4 | Hematology and clinical chemistry

Across both Phase 1 and Phase 2, white blood cell count (WBC) and individual component percentages remained within normal ranges[47,48] (Figure 4a, b). Neutrophil and lymphocyte percentages varied month-to-month, but absolute counts remained close to expected values. RBCs and platelets were in the normal range for all subjects throughout the study period (data not shown).

Liver enzymes (AST, ALT), Hemoglobin (HGB), mean corpuscular volume (MCV), hematocrit (HCT), urea nitrogen (BUN),
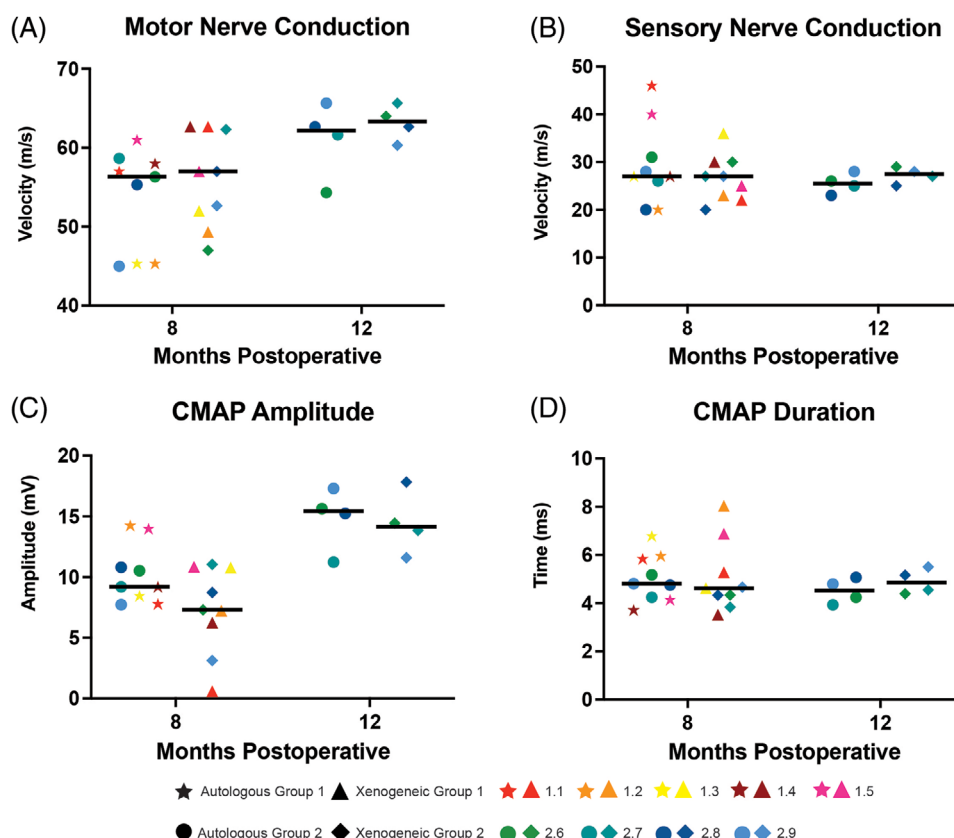
FIGURE 3 Phase 2 electrophysiological data. (A) Motor nerve conduction velocities increased from Phase 1 values and continued to increase between 8 and 12-months. Stars represent autologous treated limbs within group 1, while triangles represent xenogeneic treated limbs in group 1. Circles represent autologous treated limbs within group 2, while diamonds represent xenogeneic treated limbs in group 2. Each color represents an individual subject's data. (B) Sensory nerve conduction velocities increased from Phase 1, but appeared to plateau at 8-months. (C) Compound muscle action potential (CMAP) amplitudes increased from 5-months and continued to increase in magnitude from 8 to 12-months, approaching preoperative values, in all limbs regardless of transplant type. (D) Negligible changes in CMAP duration values were observed between 8 and 12 months.

creatinine (CREA), and electrolyte levels were stable at expected baseline levels for the duration of the study (Figure S1). Glucose (GLU) levels were above expected values and were elevated for all months except zero and twelve. We expect this was due to the recipients' increased sugar consumption during radial nerve functional evaluations. These results were reviewed by the study veterinarian.

3.5 | Pathology

Spleen, liver, heart, kidney, and lung sections obtained at necropsy were stained with H&E and assessed microscopically. All organs were determined to be consistent with normal primate organs.

3.6 | Immunogenicity

Total IgM levels were slightly elevated above preoperative levels at one or more postoperative time points in all recipients (Figure 4c). The highest level of total IgM and IgG were observed 1-month postoperative.

Overall, changes detected in total serum IgM and IgG levels did not vary more than 50% from baseline levels for each individual recipient in Groups 1 and 2 and remained stable over the course of the 12-month study.

Anti-porcine IgM and IgG levels showed an increase above preoperative levels following transplantation, followed by a gradual decrease (Figure 4d). The IgM increased to its highest level for all recipients at 1 month and remained elevated for 6-months, returning to baseline after that timepoint. Anti-porcine IgG increased to a peak at 1 and 3 months, gradually decreasing but remained significantly elevated, 5.4 fold above baseline throughout 12 months. A comparison rMFIs of the anti-porcine IgG for fresh versus frozen at 1 month and 6 months shows a higher rMFI for subjects receiving the frozen nerve but the difference was not significant, $p = .29$ and $p = .37$, respectively (Table S3).

The specificity of the anti-porcine IgG has not been addressed at this time, although others have detected high levels of anti-non-αGal in burn patients after being treated with pig-skin dressings. A nonhuman sialic acid Neu5Gc was identified as one of the target antigens.[40] Since the porcine nerve structure was in vivo for up to a year, it is possible a number of additional epitopes could also be targets.
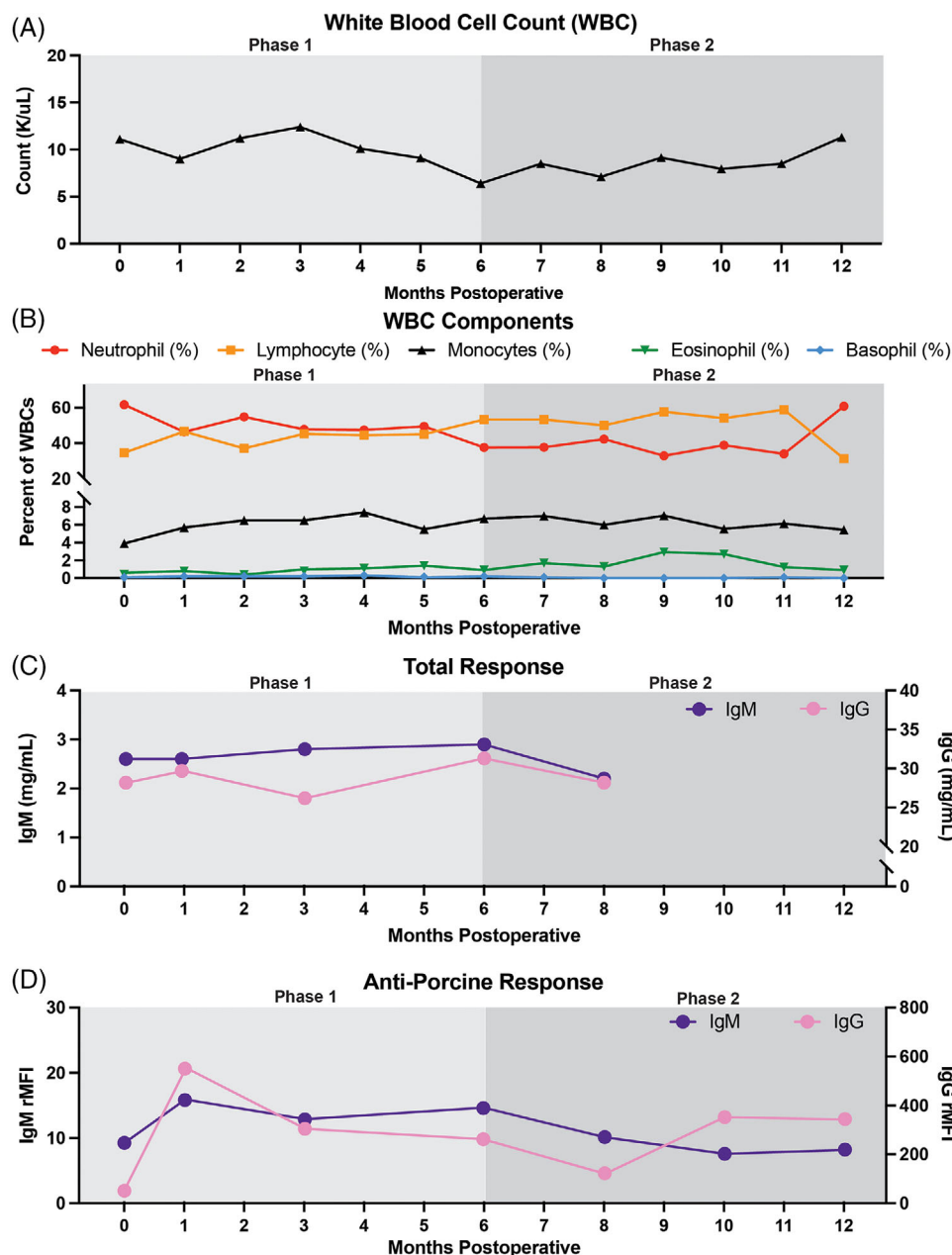
FIGURE 4 Immunogenicity following nerve reconstruction with xenogeneic nerve transplant. (A) Overall, white blood cell count (WBC) remained at expected values for the entirety of the study. (B) Composition of WBC populations remained within expected proportional ranges for the entirety of the study. (C) Total IgM and IgG titer levels did not exceed variations of greater than ±50% of baseline levels for all recipients over the course of the entire study. Data not available at 12-months for recipients in Group 2. (D) Anti-Porcine IgM and IgG responses increased the greatest at 1-month postoperative and demonstrated a gradual decrease by 8 and 12-months, respectively. Anti-porcine IgG levels remained elevated compared to preoperative levels.

3.7 | Histology

Blinded histological analysis found no meaningful differences between nerve tissue excised from transplantation sites in limbs treated with either autologous or xenogeneic transplants.

The pathologist scored the nerve bundle diameters and perioperative explanted autologous nerves not used for transplantation were positive controls with scores 4, >300 μm. For Group 1, the diameter of the regenerated nerve bundles across the defect site for all five recipients was comparable for both types of nerve transplants with scores of 2 and 3100 to 300 μm. At the end of study for Group 2 subjects, xenogeneic nerve bundle diameters scored more 2s,100–200 μm, and appeared smaller than those of the autologous control, with four autologous controls with scores of 4, >300μm and reaching preoperative diameters (Figure 5a, b).
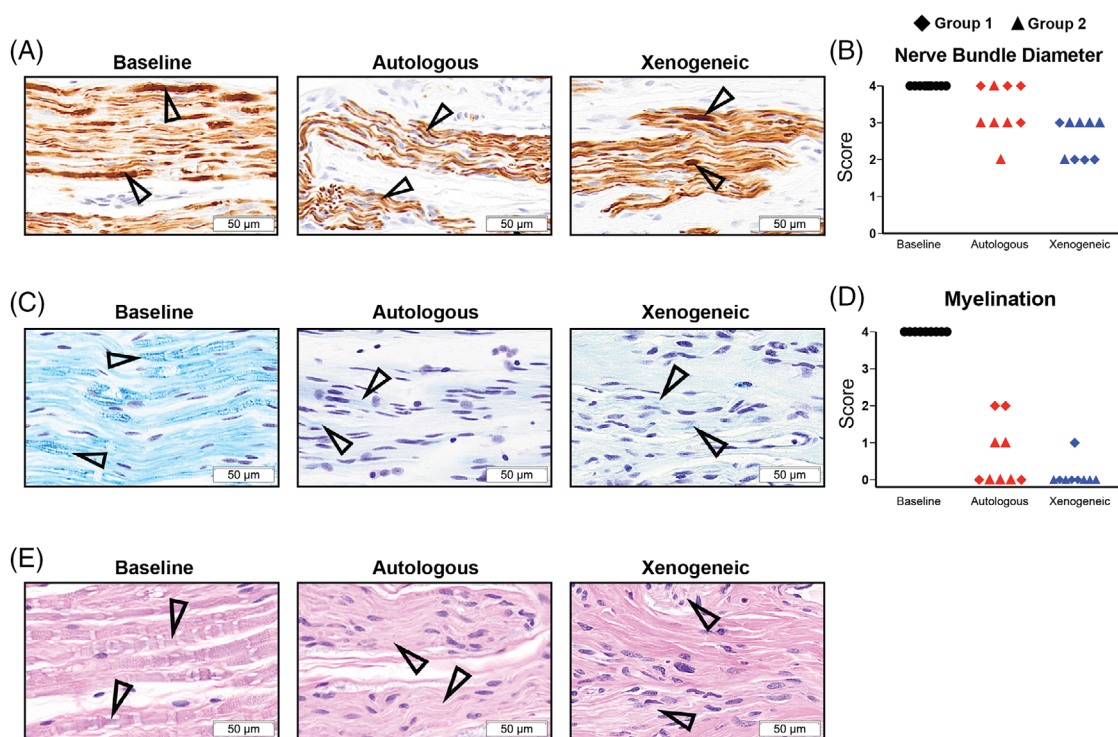
FIGURE 5 Histopathologic analysis of regenerated radial nerves. (A) Histology sections stained by immunohistochemistry for expression of neurofilament H. Arrowheads indicate axonal material. Representative images of native radial nerve at baseline and explanted nerve samples obtained at necropsy from the regenerated nerve in both autologous and xenogeneic transplanted limbs. (B) Nerve bundle diameters of the regenerated nerve from both transplant types were smaller than the diameters of native nerve obtained perioperatively and qualitatively equivalent between the two transplant types. Higher scores indicate larger diameters. (C) Luxol fast blue (LFB) staining was performed to assess the degree of myelination of regenerated nerve. Arrowheads indicate myelin. (D) A reduction in the presence of myelin was observed in all regenerated nerves compared to baseline levels, favoring limbs treated with the autologous transplant. Higher score indicates a greater presence of myelin. (E) Nerves were assessed using hematoxylin and eosin (H&E) staining. Arrowheads indicate nerve bundles.

Overall, for all recipients and transplant types, full myelination in the nerve regions immediately proximal to the transplanted sites was observed, with discernible loss of myelin in regions distal to the transplants. For xenogeneic transplants, little to no myelination was observed in subjects from either group. Overall, autologous transplants appeared to result in regenerated nerves with a greater presence of myelination (Figure 5c, d).

Macroscopic enlargement of the nerves was observed at the proximal and distal anastomotic sites for both types of transplants in all recipients (Figure 6a, b). In the transplanted regions, there was mild fibrosis with embedded nerve fibers coursing mostly longitudinally along the long axis of the transplant. The extent of the fibrous tissue present was consistent with the damage incurred as a result of the surgical procedure. Microscopic examination demonstrated foreign body reaction around the sutures, as well as multidirectional proliferation of small diameter nerve branches causing minor neuroma formation on all transplants, smaller in scale than that of the one surgical transplant failure.

There was a notable difference in the infiltration of inflammatory cells at the transplant sites between xeno- and auto- reconstituted limbs. At 8-months, the overall inflammation for the autologous treated limbs was observed to be minimal with scattered lymphocytes and

macrophages (Figure 6c). In contrast, the xenogeneic transplantation sites had a greater degree of inflammation consisting of lymphocytes and macrophages with prominent lymphoid follicles. (Figure 6d, e). By the 12-month time point, the difference in inflammation was not as prominent in the xenogeneic treatment group with minimal to mild overall inflammation attributable to the presence of lymphoid follicles along with scattered lymphocytes and macrophages, and autologous treatment group had scattered lymphocytes and macrophages.

3.8 | Biodistribution of porcine tissue in autografts and xenografts

Chimerism and PERV copy number and expression were analyzed to assess the presence of porcine cells by both conventional and Q-PCR. Samples analyzed included xenogeneic and autologous nerve tissues harvested at 8- and 12-months postoperative, sera and PBMCs from the 10 subjects obtained at various time points over the 12-month study, and spleen, kidney, liver, heart, and lung samples obtained at necropsy. Recipient PBMCs, sera, and tissues tested negative for PERV RNA and/or DNA amplification or microchimerism, indicating that
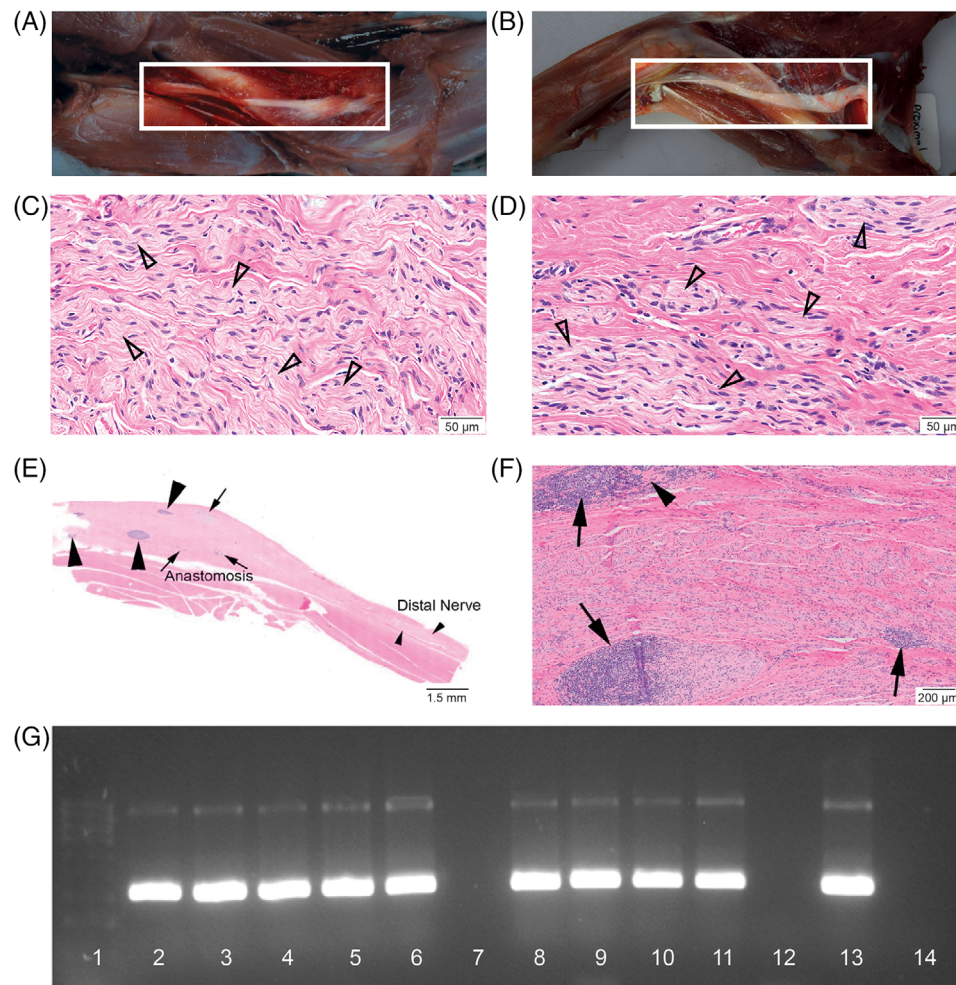
FIGURE 6 Cellular infiltrates, lymphoid follicles, and complete elimination of porcine material. (A) Autologous treated limb at necropsy (12-months postoperative) demonstrating neuroma enlargement at anastomotic sites, expected as a result of the nerve repair surgery. (B) Xenogeneic treated limb with similar presentation as seen in limbs treated with the autologous transplant. (C and D) Representative histological images from sectioned regenerated nerve; left from autologous treated limb, xenogeneic on the right. Arrowheads indicate nerve bundles. (E) Low Power showing prominent tertiary lymphoid follicles, surrounded by cell populations of lymphocytes and macrophages infiltrating the regenerated nerve from a limb treated with the xenogeneic transplant. Large arrowheads indicate lymphoid nodules in graft region. Small arrowheads indicate distal nerve. (F) High Power showing prominent tertiary lymphoid follicles, surrounded by cell populations of lymphocytes and macrophages infiltrating the regenerated nerve from a limb treated with the xenogeneic transplant. Arrows indicate lymphoid nodules. Arrowhead indicates residual graft material. (G) Qualitative PCR using primate-specific gene target demonstrates the presence of primate cells and the absence of porcine cells at transplant sites repaired with autologous (lanes 2–6) and xenogeneic transplants (lanes 8–11). Lane 12 is the negative control, lane 13 is the primate control, and lane 14 is porcine control. PCR for the housekeeping gene RPL13 was positive in all lanes (Figure S2).

there was no evidence of microchimerism or circulating porcine cells in any of the tissues/cells analyzed. Sera was also found negative for PERV RNA expression indicating that no active replication appeared to be taking place. All samples were positive for either the internal positive control (sera) or the control 18s housekeeping gene, indicating the validity of the analysis (Table 2).

As expected, the autologous nerve grafts lacked the presence of PERV or porcine cells. Surprisingly, the xenogeneic sites were also negative for the presence of porcine cells by Q-PCR, suggesting there was no residual porcine tissue in the xenogeneic nerve tissue tested. Q-PCR for porcine centromeric DNA was also negative (Table 2). However, the use of a primate-specific primer set using conventional PCR

demonstrated the presence of primate cells in both autologous and xenogeneic transplants (Figures 6g and S2).

4 | DISCUSSION

Physical guidance and Schwann cell activity are vital components of nerve repair, and optimal axonal regeneration depends on growth in a conducive and complex biological environment. Thus, the therapeutic capacity of any nerve conduit, especially one sourced from a foreign species, is correlated to its ability to mirror the physiological conditions of the host environment.

TABLE 2 PERV and porcine centromeric DNA to detect presence of porcine cells

Sample	Target centromeric porcine	Target PERV	Target 18s (mean C_T)	C_T SD
A3002	Undetected	Undetected	27.24	0.07
A3101	Undetected	Undetected	26.89	0.06
A3103	Undetected	Undetected	26.86	0.06
A4003	Undetected	Undetected	28.00	0.04
A4101	Undetected	Undetected	27.70	0.27
X3002	Undetected	Undetected	26.72	0.81
X3101	Undetected	Undetected	27.13	0.08
X3103	Undetected	Undetected	27.41	0.06
X4003	Undetected	Undetected	28.58	0.34
X4101	Undetected	Undetected	27.32	0.04

Autografts and Xenografts were tested for the presence of PERV and porcine centromeric DNA to confirm the presence of porcine cells at the end of the experiment. 18s was utilized as an internal control to confirm the validity of the Q-PCR. Ct values were consistent with the presence of DNA and indicated no inhibition in the analysis.

Porcine nerves are well suited for this task, as many essential properties are conserved, closely resembling the neuroanatomy of humans. Characterization studies reveal length, number, pattern, and fascicular area to be comparable.[1,17,27,50–53] This is highly favorable as endoneurial alignment and matched fascicular cross-sectional areas improve clinical outcomes. The architecture, composition, and distribution of essential components of the porcine ECM, such as collagen, laminin, fibronectin, and GAGs such as hyaluronic acid and chondroitin-4-sulfate are also highly similar,[20,54] resulting in clinically advantageous structural integrity, Young's modulus, and tensile strengths.[17,27] These characteristics allow for enhanced reliability of sutures to maintain stable coaptation under tension. Location and quantities of Schwann cells distributed throughout the perineurium and endoneurium of porcine peripheral nerves closely mirror that of human nerves.[55]

The regrown peripheral nerve in limbs treated with the xenogeneic transplant was capable of reinnervation of the extensor digitalis, allowing functional recovery and similar electrophysiological and morphological outcomes as the autologous control. Recovery of compound muscle action potentials and conduction velocities indicate adequately myelinated, fast-conducting fibers were restored, suggesting a successful mixed-modal repair which would be expected to improve over time.[2] The neuro-regenerative capacity observed in this study suggests that the xenogeneic transplant was able to sufficiently replicate favorable regenerative conditions, including the presence and activity of Schwann cells,[22,56–60] and other repair mechanisms, despite its foreign origin.[20,54,61,62]

The surgeries required to introduce and repair the 20 bilateral injuries required 10 surgical days in total, in addition to the surgical procurement of the porcine sciatic nerve. Over this time, uncertainty regarding the viability of the fresh nerve tissue over a 2-week period was an inherent challenge to an experimental design involving 10 subjects. The use of fresh nerve material procured from multiple source animals would introduce donor-to-donor variability and present an ethical conflict regarding the use and welfare of research animals. Cryopreservation is a well-characterized process that is recognized to preserve cell viability, basal lamina, and endoneurial structures, and its acceptable impact to tissue viability is supported in the literature.[11,14,63–65] As a result, we chose to cryopreserve the materials intended for use in 5 subjects to provide the greatest achievable standardization given these limitations, as well as additional time necessary to maintain quality and consistency with respect to surgical personnel, techniques, and conditions. Cryopreservation of xenogeneic skin transplants has also been shown to be safe and effective for up to 7 years,[66] demonstrating no significant or meaningful differences between fresh and frozen transplants.

Tacrolimus is the most widely used immunosuppressive in nerve allo-transplantation,[2,23,67–71] and use of tacrolimus in this study was due to its reported positive impact on nerve regeneration,[2,46,63,67,72–79] as well as mitigation of immunological rejection of the xenogeneic transplant. However, conversion of human clinical regimens for use in non-human primates was complicated by the variability of published protocols reported from other investigators.[2,23,67–71] In consultation with veterinarians, IACUC, and other investigators familiar with the use of tacrolimus and research involving non-human primates, the regimen used in this study was believed to be appropriate and scientifically justified.[49] The presence of tertiary lymphoid nodules at the conclusion of the study, located on the regenerated nerves in xenogeneic-treated limbs, as well as the post-operative presence of non-Gal antibodies as a result of a localized immune response to the GalT-KO porcine nerve transplant.[80] The magnitude of the immune response; however, did not result in symptoms or signs related to graft rejection, attributed in part to the concomitant use of tacrolimus.[49]

The data generated post the month 8 time point has been considered not relevant by the authors, due to the afore mentioned complications with the data that would have impacted the study's statistical power. As a result, the qualitative histopathological analysis is hindered by the lack of quantitative, objective metrics, and could be improved in future studies with nerve stereology and morphometry for quantification and immunohistochemistry for specific antigens.

Finally, we expected the cellular components of the 4-cm porcine transplant to be fully replaced and repopulated by the host cells at the rate of 1 mm/day,[19,73,81] culminating in the complete, macrophage-mediated clearance of porcine cellular material and elimination of immunogenic porcine antigens. This was supported by the lack of detectable porcine DNA using Q-PCR in both the xenogeneic and autologous nerve tissue at necropsy. In addition, assessment of blood and tissue from the recipients indicated no circulating porcine cells or replication of PERV elements. Both housekeeping Q-PCR and qualitative PCR assays detected DNA in the nerve samples, however, initially it was not possible to differentiate between primate and porcine as the control assays were not specific. Conventional PCR utilizing a primate specific gene did indeed show that

primate cells were detectable in both the autologous and xenogeneic transplants.

Previous testing of skin xenotransplants had demonstrated that porcine cells were detectable at the graft site, but this did not extend to the peripheral circulation.[34] Given the lack of detection here and the immunological responses shown, this supports the hypothesis that the porcine transplant is fully replaced and repopulated by the host cells. These methods are highly sensitive and specific and are of more value than, for example, immunohistochemistry, which in addition to lack of sensitivity, can be complicated by the lack of suitable antibodies to distinguish cell content. Indeed, recently, it has been suggested that the use of PERV genes for detection increases the sensitivity of the molecular assay and may also be indicative of an inflammatory reaction in addition to testing for infection as is done for allo-transplants.[82] No significant immunological reaction was seen in these animals again reflected in the lack of detection. While Rhesus Macaques are currently not considered a suitable model for PERV infection,[83] this limitation does not affect this study as our intention is to assess the presence or absence of porcine cells using the best tools possible.

These limitations withstanding, this pilot study delivers data of high interest for the field. Combined, our long-term, in vivo data presented herein suggests promise for the repair of large-gap PNIs via the use of viable, GalT-KO porcine nerve transplants. Motor nerve conduction velocity showed partial recovery in all subjects, with the limbs treated with the xenogeneic transplant exhibiting greater recovery. Clinical data has demonstrated positive functional outcomes in the repair of peripheral nerve injuries of up to 70 mm in length using acellular allograft nerves.[84] However, in large-gap injuries, the regenerative capacity of acellular nerve allografts has shown to be limited, believed to be due in part to increased Schwann cell senescence over long distances.[11,57,62,85] Further rigorous evaluation is required, but the similarity in functional outcomes between the cryopreserved xenogeneic and autologous nerve transplants suggest positive implications for the future translation of cryopreserved xenogeneic nerve transplant in human clinical application.

5 | CONCLUSION

The field of allo-transplantation has been a success of modern medicine, has been hindered by numerous shortcomings.[1-3] Xenotransplantation offers an attractive alternative solution, and the field has advanced significantly in the past three decades. While permanent, solid organ xenotransplantation remains elusive at this time, our findings in this pilot study suggest a promising potential for therapeutic neural xenotransplants that are ultimately eliminated via natural endogenous processes but provide meaningful interim clinical, and potentially long-term benefit. The therapeutic success of such consumable xenogeneic materials has recently been demonstrated in human clinical trials of cryopreserved split-thickness skin xenotransplants for the treatment of severe burns. Critical foundational translational aspects of this program, such as patient monitoring for zoonosis and immunogenicity, as well as regulatory requirements and ethical considerations related to animal transplant donors, can be directly applied to support a broader regenerative medicine platform and suggest the future potential for the interchangeable clinical use of cross-species cells, tissues, and organs in human medicine.

AUTHOR CONTRIBUTIONS

P.H., C.L.C., and R.M. obtained the funding and designed the experiments. P.H. and C.L.C. performed all animal surgeries. A.L. provided the animal facilities, resources, veterinary observations, and performed behavioral experiments, hematology, and clinical chemistry. M.M. performed electrophysiology. L.S., J.T., and N.G. performed PERV analysis and all PCR. J.W. performed all pathology. B.O. and A.L. performed immunogenicity assays. P.H., E.J.C., D.L., M.M., J.W., B.O., L.S., and R.M. performed data analysis. D.L. and E.J.C. drafted the manuscript. S.G., J.D., and all authors revised the manuscript for critical content. P.H., K.R., and J.A. managed all administrative, technical, or supervisory tasks.

ACKNOWLEDGMENTS

COFLICT OF INTEREST

ORCID

Elizabeth J. Chang https://orcid.org/0000-0002-5966-6531
Kaitlyn Rogers https://orcid.org/0000-0001-9079-5326
Jamie Tarlton https://orcid.org/0000-0003-2451-8958
Linda Scobie https://orcid.org/0000-0002-0727-7163

REFERENCES

1. Zilic L, Garner PE, Yu T, Roman S, Haycock JW, Wilshaw S-P. An anatomical study of porcine peripheral nerve and its potential use in nerve tissue engineering. *J Anat*. 2015;227(3):302-314. https://doi.org/10.1111/joa.12341
2. Grinsell D, Keating CP. Peripheral nerve reconstruction after injury: a review of clinical and experimental therapies. *BioMed Res Int*. 2014;2014:698256. https://doi.org/10.1155/2014/698256

3. Johnson EO, Soucacos PN. Nerve repair: experimental and clinical evaluation of biodegradable artificial nerve guides. *Injury*. 2008;39(3):30-36. https://doi.org/10.1016/j.injury.2008.05.018

4. Li R, Liu Z, Pan Y, Chen L, Zhang Z, Lu L. Peripheral nerve injuries treatment: a systematic review. *Cell Biochem Biophys*. 2014;68(3):449-454. https://doi.org/10.1007/s12013-013-9742-1

5. Vasileiadis A. Bridging of peripheral nerve defects by autologous nerve grafting personal experience. *MOJ Orthop Rheumatol*. 2016;5(3). doi: http://10.15406/mojor.2016.05.00183

6. Lee SK, Wolfe SW. Peripheral nerve injury and repair. *JAAOS - J Am Acad Orthop Surg*. 2000;8(4):243-252.

7. Griffin JW, Hogan MV, Chhabra AB, Deal DN. Peripheral nerve repair and reconstruction. *J Bone Joint Surg Am*. 2013;95(23):2144-2151. https://doi.org/10.2106/JBJS.L.00704

8. Uranues S, Bretthauer G, Tomasch G, et al. A new synthetic conduit for the treatment of peripheral nerve injuries. *World J Surg*. 2020;44(10):3373-3382. https://doi.org/10.1007/s00268-020-05620-0

9. Bittner GD, Schallert T, Peduzzi JD. Degeneration, trophic interactions, and repair of severed axons: a reconsideration of some common assumptions. *Neuroscientist*. 2000;6(2):88-109. https://doi.org/10.1177/107385840000600207

10. Wagstaff LJ, Gomez-Sanchez JA, Fazal SV, et al. Failures of nerve regeneration caused by aging or chronic denervation are rescued by restoring Schwann cell c-Jun. *eLife*. 2021;10:e62232. https://doi.org/10.7554/eLife.62232

11. Squintani G, Bonetti B, Paolin A, et al. Nerve regeneration across cryopreserved allografts from cadaveric donors: a novel approach for peripheral nerve reconstruction. *J Neurosurg*. 2013;119(4):907-913. https://doi.org/10.3171/2013.6.JNS121801

12. Pfister BJ, Gordon T, Loverde JR, Kochar AS, Mackinnon SE, Cullen DK. Biomedical engineering strategies for peripheral nerve repair: surgical applications, state of the art, and future challenges. *Crit Rev Biomed Eng*. 2011;39(2):81-124. https://doi.org/10.1615/critrevbiomedeng.v39.i2.20

13. Zilic L. Development of Acellular Porcine Peripheral Nerves. phd. University of Sheffield; 2016. Accessed November 9, 2021. https://etheses.whiterose.ac.uk/15777/

14. Evans PJ, Mackinnon SE, Levi ADO, et al. Cold preserved nerve allografts: changes in basement membrane, viability, immunogenicity, and regeneration. *Muscle Nerve*. 1998;21(11):1507-1522. https://doi.org/10.1002/(SICI)1097-4598(199811)21:11<1507::AID-MUS21>3.0.CO;2-W

15. Siemionow M, Brzezicki G. Chapter 8: current techniques and concepts in peripheral nerve repair. *Int Rev Neurobiol*. 2009;87:141-172. https://doi.org/10.1016/S0074-7742(09)87008-6

16. Lanier ST, Jordan SW, Ko JH, Dumanian GA. Targeted muscle reinnervation as a solution for nerve pain. *Plast Reconstr Surg*. 2020;146(5):651e. https://doi.org/10.1097/PRS.0000000000007235

17. Sunderland SS. The anatomy and physiology of nerve injury. *Muscle Nerve*. 1990;13(9):771-784. https://doi.org/10.1002/mus.880130903

18. Saffari T, Bedar M, Hundepool C, Bishop A, Shin A. The role of vascularization in nerve regeneration of nerve graft. *Neural Regen Res*. 2020;15(9):1573-1579. https://doi.org/10.4103/1673-5374.276327

19. Evans PJ, Midha R, Mackinnon SE. The peripheral nerve allograft: A comprehensive review of regeneration and neuroimmunology. *Prog Neurobiol*. 1994;43(3):187-233. https://doi.org/10.1016/0301-0082(94)90001-9

20. Ide C, Osawa T, Tohyama K. Nerve regeneration through allogeneic nerve grafts, with special reference to the role of the schwann cell basal lamina. *Prog Neurobiol*. 1990;34(1):1-38. https://doi.org/10.1016/0301-0082(90)90024-B

21. Cooper DKC, Ezzelarab MB, Hara H. Low anti-pig antibody levels are key to the success of solid organ xenotransplantation: but is this sufficient? *Xenotransplantation*. 2017;24(6). https://doi.org/10.1111/xen.12360

22. Rutten MJ, Janes MA, Chang IR, Gregory CR, Gregory KW. Development of a functional schwann cell phenotype from autologous porcine bone marrow mononuclear cells for nerve repair. *Stem Cells Int*. 2012;2012:738484. https://doi.org/10.1155/2012/738484

23. Hebebrand D, Zohman G, Jones NF. Nerve xenograft transplantation. Immunosuppression with FK-506 and RS-61443. *J Hand Surg Edinb Scotl*. 1997;22(3):304-307. https://doi.org/10.1016/s0266-7681(97)80391-9

24. Lin SS, Kooyman DL, Daniels LJ, et al. The role of natural anti-gal antibodies in hyperacute rejection of pig-to-baboob ardia xenotransplants. *Transpl Immunol*. 1995;5(3):212-218.

25. Adigbli G, Ménoret S, Cross AR, Hester J, Issa F, Anegon I. Humanization of immunodeficient animals for the modeling of transplantation, graft versus host disease, and regenerative medicine. *Transplantation*. 2020;104(11):2290-2306. https://doi.org/10.1097/TP.0000000000003177

26. Spitaleri G, Farrero M. Translational medicine in brain stem death and heart transplantation. *Transplantation*. 2020;104(11):2258-2259. https://doi.org/10.1097/TP.0000000000003218

27. Burrell JC, Browne KD, Dutton JL, et al. A porcine model of peripheral nerve injury enabling ultra-long regenerative distances: surgical approach, recovery kinetics, and clinical relevance. *bioRxiv*. Published online April 16, 2019:610147. https://doi.org/10.1101/610147

28. Lunney JK, Ho C-S, Wysocki M, Smith DM. Molecular genetics of the swine major histocompatbility complex, the SLA complex. *Dev Comp Immunol*. 2009;33(3):362-374. https://doi.org/10.1016/j.dci.2008.07.002

29. Denner J, Paving the path toward porcine organs for transplantation. In Phimister EG, ed. *N Engl J Med*. 2017;377(19):1891-1893.

30. Argaw T, Colon-Moran W, Wilson C. Susceptibility of porcine endogenous retrovirus to anti-retroviral inhibitors. *Xenotransplantation*. 2016;23(2):151-158. https://doi.org/10.1111/xen.12230

31. Demange A, Yajjou-Hamalian H, Gallay K, et al. Porcine endogenous retrovirus-A/C: biochemical properties of its integrase and susceptibility to raltegravir. *J Gen Virol*. 2015;96(10):3124-3130.

32. Cowan PJ, Tector AJ. The resurgence of xenotransplantation. *Am J Transplant*. 2017;17(10):2531-2536. https://doi.org/10.1111/ajt.14311

33. Fishman JA, Scobie L, Takeuchi Y. Xenotransplantation-associated infectious risk: a WHO consultation: xenotransplantation-associated infectious risk. *Xenotransplantation*. 2012;19(2):72-81. https://doi.org/10.1111/j.1399-3089.2012.00693.x

34. Holzer PW, Chang E, Wicks J, Scobie L, Crossan C, Monroy R. Immunological response in cynomolgus macaques to porcine α-1,3 galactosyltransferase knockout viable skin xenotransplants–A pre-clinical study. *Xenotransplantation*. 2020;27(6):e12632. https://doi.org/10.1111/xen.12632

35. Wang LH, Weiss MD. Anatomical, clinical, and electrodiagnostic features of radial neuropathies. *Phys Med Rehabil Clin N Am*. 2013;24(1):33-47. https://doi.org/10.1016/j.pmr.2012.08.018

36. Holzer P, Adkins J, Moulton K, Zhu L, Monroy R, Cetrulo CL. Vital, porcine, gal-knockout skin transplants provide efficacious temporary closure of full-thickness wounds: good laboratory practice-compliant studies in nonhuman primates. *J Burn Care Res Off Publ Am Burn Assoc*. 2020;41(2):229-240. https://doi.org/10.1093/jbcr/irz124

37. Althagafi A, Nadi M. Acute nerve injury. *StatPearls*. StatPearls Publishing; 2021. Accessed April 21, 2021. http://www.ncbi.nlm.nih.gov/books/NBK549848/

38. Arora S, Goel N, Cheema GS, Batra S, Maini L. A method to localize the radial nerve using the 'Apex Of Triceps Aponeurosis' as a landmark. *Clin Orthop*. 2011;469(9):2638-2644. https://doi.org/10.1007/s11999-011-1791-4

39. Biomere. PRT18-01 Neurography Audited Report; 2019.

40. Scobie L, Padler-Karavani V, Le Bas-Bernardet S, et al. Long-term IgG response to porcine Neu5Gc antigens without transmission of PERV in burn patients treated with porcine skin xenografts. *J Immunol*. 2013;191(6):2907-2915. https://doi.org/10.4049/jimmunol.1301195

41. Tripathi V, Obermann WMJ. A primate specific extra domain in the molecular chaperone Hsp90. *Plos One*. 2013;8(8):e71856. https://doi.org/10.1371/journal.pone.0071856

42. Wang D, Huang X, Fu G, et al. A simple model of radial nerve injury in the rhesus monkey to evaluate peripheral nerve repair. *Neural Regen Res*. 2014;9(10):1041. https://doi.org/10.4103/1673-5374.133166

43. Injury of Radial Nerve: Causes, Symptoms & Diagnosis. Healthline. Published September 26, 2015. Accessed August 3, 2021. https://www.healthline.com/health/radial-nerve-dysfunction

44. Gragossian A, Varacallo M. Radial nerve injury. *StatPearls*. StatPearls Publishing; 2021. Accessed August 3, 2021. http://www.ncbi.nlm.nih.gov/books/NBK537304/

45. Mohanna P-N, Young RC, Wiberg M, Terenghi G. A composite poly-hydroxybutyrate-glial growth factor conduit for long nerve gap repairs. *J Anat*. 2003;203(6):553-565. https://doi.org/10.1046/j.1469-7580.2003.00243.x

46. Chunasuwankul R, Ayrout C, Dereli Z, Gal A, Lanzetta M, Owen E. Low dose discontinued FK506 treatment enhances peripheral nerve regeneration. *Int Surg*. 2002;87(4):274-278.

47. Koo B-S, Lee D-Ho, Kang P, et al. Reference values of hematological and biochemical parameters in young-adult cynomolgus monkey (Macaca fascicularis) and rhesus monkey (Macaca mulatta) anesthetized with ketamine hydrochloride. *Lab Anim Res*. 2019;35(1):7. https://doi.org/10.1186/s42826-019-0006-0

48. Chen Y, Qin S, Ding Y, et al. Reference values of clinical chemistry and hematology parameters in rhesus monkeys (Macaca mulatta). *Xenotransplantation*. 2009;16(6):496-501. https://doi.org/10.1111/j.1399-3089.2009.00554.x

49. Tacrolimus (Oral Route) Proper Use - Mayo Clinic. Accessed October 28, 2021. https://www.mayoclinic.org/drugs-supplements/tacrolimus-oral-route/proper-use/drg-20068314

50. Chentanez V, Cha-oumphol P, Kaewsema A, Agthong S, Huanmanop T. Morphometric data of normal sural nerve in Thai adults. *J Med Assoc Thail Chotmaihet Thangphaet*. 2006;89(5):670-674.

51. Ugrenović S, Topalović M, Jovanović I, Antović A, Milić M, Ignjatović A. Morphological and morphometric analysis of fascicular structure of tibial and common peroneal nerves. *Med Biol*. 2014;16(1):18-22.

52. Ugrenovic SZ, Jovanovic ID, Kovacevic P, Petrović S, Simic T. Similarities and dissimilarities of the blood supplies of the human sciatic, tibial, and common peroneal nerves. *Clin Anat*. 2013;26(7):875-882. https://doi.org/10.1002/ca.22135

53. Gustafson KJ, Grinberg Y, Joseph S, Triolo RJ. Human distal sciatic nerve fascicular anatomy: Implications for ankle control using nerve-cuff electrodes. *J Rehabil Res Dev*. 2012;49(2):309-321.

54. Zhang Y, Luo H, Zhang Z, et al. A nerve graft constructed with xenogeneic acellular nerve matrix and autologous adipose-derived mesenchymal stem cells. *Biomaterials*. 2010;31(20):5312-5324. https://doi.org/10.1016/j.biomaterials.2010.03.029

55. Bhatheja K, Field J. Schwann cells: Origins and role in axonal maintenance and regeneration. *Int J Biochem Cell Biol*. 2006;38(12):1995-1999. https://doi.org/10.1016/j.biocel.2006.05.007

56. Whitlock EL, Tuffaha SH, Luciano JP, et al. Processed allografts and type I collagen conduits for repair of peripheral nerve gaps. *Muscle Nerve*. 2009;39(6):787-799. https://doi.org/10.1002/mus.21220

57. Weber RA, Breidenbach WC, Brown RE, et al. A randomized prospective study of polyglycolic acid conduits for digital nerve reconstruction in humans. *Plast Reconstr Surg*. 2000;106(5):1036-1045; discussion 1046-1048. https://doi.org/10.1097/00006534-200010000-00013

58. Zalewski AA, Silvers WK An evaluation of nerve repair with nerve allografts in normal and immunologically tolerant rats. *J Neurosurg*. 1980;52(4):557-563. https://doi.org/10.3171/jns.1980.52.4.0557

59. Quintes S, Goebbels S, Saher G, Schwab MH, Nave K-A. Neuron-glia signaling and the protection of axon function by Schwann cells. *J Peripher Nerv Syst*. 2010;15(1):10-16. https://doi.org/10.1111/j.1529-8027.2010.00247.x

60. Nave K-A, Trapp BD. Axon-glial signaling and the glial support of axon function | annual review of neuroscience. *Annu Rev Neurosci*. 2008;31:535-561. Accessed November 2, 2021. https://www-annualreviews-org.ezproxy.neu.edu/doi/10.1146/annurev.neuro.30.051606.094309

61. Hudson TW, Zawko S, Deister C, et al. Engineering an improved acellular nerve graft via optimized chemical processing. *Tissue Eng*. 2004;10(9-10):1346-1358. https://doi.org/10.1089/ten.2004.10.1641

62. Saheb-Al-Zamani M, Yan Y, Farber SJ, et al. Limited regeneration in long acellular nerve allografts is associated with increased Schwann cell senescence. *Exp Neurol*. 2013;247:165-177. https://doi.org/10.1016/j.expneurol.2013.04.011

63. Aubá C, Hontanilla B, Arcocha J, Gorría Ó. Peripheral nerve regeneration through allografts compared with autografts in FK506-treated monkeys. *J Neurosurg*. 2006;105(4):602-609. https://doi.org/10.3171/jns.2006.105.4.602

64. Fansa H, Lassner F, Kook PH, Keilhoff G, Schneider W. Cryopreservation of peripheral nerve grafts. *Muscle Nerve*. 2000;23(8):1227-1233. https://doi.org/10.1002/1097-4598(200008)23:8⟨1227::AID-MUS11⟩3.0.CO;2-6

65. Grand AG, Myckatyn TM, Mackinnon SE, Hunter DA. Axonal regeneration after cold preservation of nerve allografts and immunosuppression with tacrolimus in mice. *J Neurosurg*. 2002;96(5):924-932. https://doi.org/10.3171/jns.2002.96.5.0924

66. Holzer PW, Leonard DA, Shanmugarajah K, et al. A comparative examination of the clinical outcome and histological appearance of cryopreserved and fresh split-thickness skin grafts. *J Burn Care Res Off Publ Am Burn Assoc*. 2017;38(1):e55-e61. https://doi.org/10.1097/BCR.0000000000000431

67. Gold Bg, Katoh K, Storm-Dickerson T. The immunosuppressant FK506 increases the rate of axonal regeneration in rat sciatic nerve. *J Neurosci*. 1995;15(11):7509-7516. https://doi.org/10.1523/JNEUROSCI.15-11-07509.1995

68. Kornfeld T, Vogt PM, Radtke C. Nerve grafting for peripheral nerve injuries with extended defect sizes. *Wien Med Wochenschr*. 2019;169(9-10):240-251. https://doi.org/10.1007/s10354-018-0675-6

69. Mackinnon SE, Doolabh VB, Novak CB, Trulock EP. Clinical Outcome following Nerve Allograft Transplantation. *Plast Reconstr Surg*. 2001;107(6):1419-1429.

70. Phan DQD, Schuind F. Tolerance and effects of FK506 (tacrolimus) on nerve regeneration: a pilot study. *J Hand Surg Eur*. 2012;37(6):537-543. https://doi.org/10.1177/1753193411427826

71. Tung TH. Tacrolimus (FK506): Safety and Applications in Reconstructive Surgery. *Hand N Y N*. 2010;5(1):1-8. https://doi.org/10.1007/s11552-009-9193-8

72. Yang RK, Lowe JB, Sobol JB, Sen SK, Hunter DA, Mackinnon SE. Dose-Dependent Effects of FK506 on Neuroregeneration in a Rat Model: *Plast Reconstr Surg*. 2003;112(7):1832-1840. https://doi.org/10.1097/01.PRS.0000091167.27303.18

73. Yan Y, Sun HH, Hunter DA, Mackinnon SE, Johnson PJ. Efficacy of Short-Term FK506 Administration on Accelerating Nerve Regeneration. *Neurorehabil Neural Repair*. 2012;26(6):570-580. https://doi.org/10.1177/1545968311431965

74. Gold BG, Storm-Dickerson T, Austin DR. The immunosuppressant FK506 increases functional recovery and nerve regeneration following peripheral nerve injury. *Restor Neurol Neurosci*. 1994;6(4):287-296. https://doi.org/10.3233/RNN-1994-6404

75. Wang MS, Zeleny-Pooley M, Gold BG. Comparative dose-dependence study of FK506 and cyclosporin A on the rate of axonal

regeneration in the rat sciatic nerve. *J Pharmacol Exp Ther.* 1997;282(2):1084-1093.

76. Kim J, Hong S, Chung H, et al. Long-term porcine islet graft survival in diabetic non-human primates treated with clinically available immunosuppressants. *Xenotransplantation (København).* 2021;28(2):e12659. https://doi.org/10.1111/xen.12659

77. Matsumoto S, Shimoda M. Current situation of clinical islet transplantation from allogeneic toward xenogeneic. *J Diabetes.* 2020;12(10):733-741. https://doi.org/10.1111/1753-0407.13041

78. Wynyard S, Nathu D, Garkavenko O, Denner J, Elliott R. Microbiological safety of the first clinical pig islet xenotransplantation trial in New Zealand. *Xenotransplantation.* 2014;21(4):309-323. https://doi.org/10.1111/xen.12102

79. Shahraki M, Mohammadi R, Najafpour A. Influence of Tacrolimus (FK506) on Nerve Regeneration Using Allografts: A Rat Sciatic Nerve Model. *J Oral Maxillofac Surg Off J Am Assoc Oral Maxillofac Surg.* 2015;73(7):1438.e1-9. https://doi.org/10.1016/j.joms.2015.03.032

80. Dor FJMF, Tseng Y-L, Cheng J, et al. alpha 1,3-Galactosyltransferase Gene-Knockout Miniature Swine Produce Natural Cytotoxic Anti-Gal Antibodies. *Transplantation.* 2004;78(1):15-20. https://doi.org/10.1097/01.TP.0000130487.68051.EB

81. Whitlock EL, Myckatyn TM, Tong AY, et al. Dynamic Quantification of Host Schwann Cell Migration into Peripheral Nerve Allografts. *Exp Neurol.* 2010;225(2):310-319. https://doi.org/10.1016/j.expneurol.2010.07.001

82. Denner J. Detection of cell-free pig DNA using integrated PERV sequences to monitor xenotransplant tissue damage and rejection. *Xenotransplantation.* 2021;28(4):e12688. https://doi.org/10.1111/xen.12688

83. Denner J. Why was PERV not transmitted during preclinical and clinical xenotransplantation trials and after inoculation of animals? *Retrovirology.* 2018;15(1):28. https://doi.org/10.1186/s12977-018-0411-8

84. Isaacs J, Safa B. A Preliminary Assessment of the Utility of Large-Caliber Processed Nerve Allografts for the Repair of Upper Extremity Nerve Injuries. *Hand N Y N.* 2017;12(1):55-59. https://doi.org/10.1177/1558944716646782

85. Safa B, Shores JT, Ingari JV, et al. Recovery of Motor Function after Mixed and Motor Nerve Repair with Processed Nerve Allograft. *Plast Reconstr Surg – Glob Open.* 2019;7(3):e2163. https://doi.org/10.1097/GOX.0000000000002163

SUPPORTING INFORMATION

Additional supporting information can be found online in the Supporting Information section at the end of this article.